ELSEVIER

Theoretical and Applied Fracture Mechanics 33 (2000) 135–143

theoretical and applied fracture mechanics

www.elsevier.com/locate/tafmec

A heuristic approach to microcracking and fracture for ceramics with statistical consideration

A. Brencich, A. Carpinteri *

Department of Structural Engineering, Politecnico di Torino, C.so Duca degli Abruzzi 24, 10129 Torino, Italy

Abstract

Microcracking damage and toughening are examined for ceramics. These effects have been found to depend on the material microstructure and macrocrack growth. Isotropic damage, attributed to random distribution of microcrack location, length and orientation can be associated with a disordered microstructure and a non-uniform residual stress field. When the applied stress is the main cause of cracking, the microcrack distribution is no longer random such as a system of quasi-parallel cracks. To highlight the effect of crack interaction, discrete models are advanced where damage is simulated by a distribution of microcracks. The dilute concentration assumption is invoked to simplify the analysis.

The two-dimensional discrete model is based on a phenomenological approach that is statistical in character. Interactions of microcracks and with a macrocrack are considered by means of a boundary element technique (A. Brencich, A. Carpinteri, Int. J. Fracture 76 (1996) 373–389; A. Brencich, A. Carpinteri, Eng. Fract. Mech. 59 (1998) 797–814) where both isotropic and anisotropic damage could be treated. Comparisons with other results are made to show that the model can be applied to analyse the fracture behaviour of different materials.

Keywords: Microcrack damage; Crack interaction; Statistical model; Microcrack toughening

1. Introduction

Brittle materials are known to contain extensive microcracks. Such a region is known as *process zone*. It is developed in front of a macrocrack [3–7]. This occurs in ceramics, rocks and concrete-like materials. Microcracking damage tends to toughen the material at the macroscopic scale level for stationary and steadily growing cracks [5,8–10]. That is the load level at which a crack propagates is increased when compared with the estimated limit load for the undamaged material.

With reference to the material microstructure, two different distributions could be identified inside the process zone. For a two-phase ceramic system, such as zirconia toughened alumina, microcracks are nucleated at grain boundaries in the form of intergranular [8] and radial cracks [9]. Due to the random distribution of the second phase particles and grain facets, the microcracks are randomly distributed and the damaged zone exhibits an isotropic behaviour. Other ceramics, such as lithium–alumino-silicate glass ceramics [5] or alumina–silicon carbide composites [10] and concrete-like materials [6,7], may be regarded as a homogeneous matrix containing dispersed second phase particles. For these materials, the microcrack pattern resembles the principal stress

* Corresponding author. Tel.: +39-11-564-4850; fax: +39-11-564-4899.

E-mail address: carpinteri@polito.it (A. Carpinteri).

0167-8442/00/$ - see front matter
PII: S0167-8442(00)00008-2

directions with some deviations due to inhomogeneities at the microscopic level. The material inside the process zone is highly anisotropic.

Microcrack toughening has been attributed to energy dissipation [11,12] and residual stress relief [8,13–15] that are associated with crack nucleation and growth. The latter corresponds to steadily growing cracks, while the onset of crack growth appears to be independent of residual stress [16].

Besides, one of the effects of the interactions between the macrocrack and the second phase particles consists of a mixed mode loading at the main crack tip which forces it to deflect away from the path it would have if the material were undamaged. Crack entrapment by material inhomogeneities [17,18] is another way of enhancing fracture resistance.

Depending on the material and loading condition, delay fracture mechanisms may not occur at the same time. Consider a cracked solid under load, removed and then re-applied in a quasi-static way. Residual stress would have then been relieved. In this case, onset of crack propagation in an alumina–silicon carbide type ceramic composite (homogeneous matrix with dispersed second phase particles) would be dictated by stress-induced microcracks in front of the main crack tips. Elastic interaction between cracks would delay crack growth [19,20].

Theoretical analysis of microcracking related to fracture behaviour of solids involves two approaches. One of them refers to average quantities describing the cracked material at a macroscopic scale [13,14,21,22]. The other approach makes use of discrete models in which the effective microcrack distribution is simulated [16,19,20,23–25].

A typical continuum model views the process zone as a region where the material properties have been degraded. The inner part of the process zone is characterised by the so-called saturated density. It is usually considered as a measure of damage that corresponds to a region where the elastic properties have degraded the most. Such an approach is admissible when random microcracking produces an isotropic process zone. A softened elastic material describes a process zone symmetric with respect to the main crack. In this way, no anti-symmetric stress field can be simulated. That is the main crack deviates away from its original path, a feature of microcracking. The anisotropic behaviour of the damaged area cannot be taken into account.

Discrete models usually follow a kinematic approach in that the crack geometry is pre-set according to some empirical or heuristic criterion. A major drawback of such schemes is that only simple geometries could be treated involving a few microcracks or periodic arrays of microcracks [26–28]. A satisfactory treatment of the process zone requires a large number of microcracks. Hence discrete models are restricted to numerical techniques [1,26,29] unless the interaction of cracks is neglected [16].

2. Mesomechanical model

Crack density [30–32] in two-dimensions can be defined in terms of a representative area A containing N_A cracks of average length $\langle 2\ell \rangle$, i.e.,

$$\rho = \frac{1}{A} N_A \langle 2\ell \rangle^2. \tag{1}$$

The surface crack density may be regarded as an average measure of damage in the microcracked areas. Experiments [3] have shown that the highest crack density occurs near the macrocrack tip and it is nearly constant. This portion of the process zone is said to be *saturated* with the maximum crack density ρ_s, as shown in Fig. 1. Microcracking

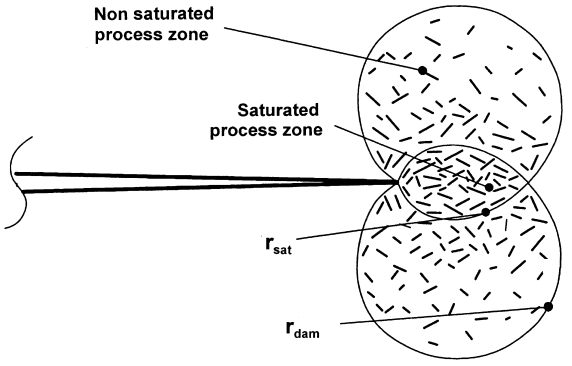

Fig. 1. Saturated and non-saturated areas inside the process zone for a stationary crack.

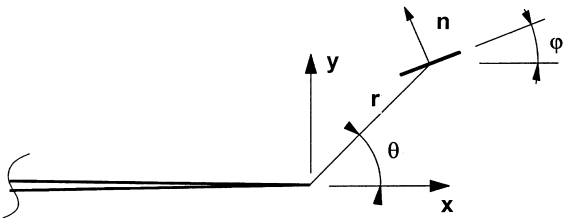

Fig. 2. Orientation of a microcrack in relation to the main crack tip.

damage and the crack density tend to decrease with increasing distance from the macrocrack tip and they vanish at the boundary where the process zone and the undamaged material are met.

The location of such a boundary can be calculated by invoking some simplifying assumptions. Consider a generic location r, ϑ at which the nucleation of a microcrack is possible, Fig. 2. Under pure Mode I loading, the normal stress in the direction of outward normal n is given by

$$\sigma_n = \frac{K_I}{\sqrt{2\pi r}}\left[\cos\frac{\vartheta}{2} + \frac{1}{2}\sin\vartheta\ \sin\left(\frac{3}{2}\vartheta - 2\varphi\right)\right]. \quad (2)$$

The microcracks could nucleate if there prevails at least one orientation φ for which σ_n exceeds a threshold limit σ_{lim}, say the tensile strength σ_t . The material will remain undamaged if none of the orientations φ fulfills this condition. Conversely, if nucleation is found for any orientation φ, then microcracks shall nucleate for all orientations. This is assumed to occur inside the saturated process zone. An intermediate situation could arise when cracks are nucleated only for $\Delta\varphi < \pi$. This is to be found in the outer portion of the process zone.

2.1. Crack density

An analytical expression of crack density in this area as a function of the vertical distance y from the microcrack line (Fig. 2) can be obtained by assuming that ρ is directly proportional to $\Delta\varphi$ [2,16]

$$\rho = \frac{\rho_{sat}}{\pi}\cos^{-1}\left[\frac{\sigma_{lim}}{K_I}\sqrt{8\pi y} - \sqrt{2}\right]. \quad (3)$$

The outer boundary of the saturated area corresponds to the location where the minimum normal stress σ_n equals the limit stress σ_{lim}

$$r_{sat}(\vartheta) = \left(\frac{K_I}{\sigma_{lim}}\right)^2 \frac{1}{2\pi}\left(\cos\frac{\vartheta}{2} - \frac{1}{2}\sin\vartheta\right)^2. \quad (4)$$

The outer boundary of the previous zone is where the maximum value of σ_n equals σ_{lim}. This gives

$$r_{dam}(\vartheta) = \left(\frac{K_I}{\sigma_{lim}}\right)^2 \frac{1}{2\pi}\left(\cos\frac{\vartheta}{2} + \frac{1}{2}\sin\vartheta\right)^2. \quad (5)$$

The analytical details and assumptions are given in [2].

In the saturated area of the process zone, nucleation is possible for every orientation φ. The actual microcracking will depend on the material microstructure. If the material can be regarded as homogeneous at the scale under consideration, then a crack would be assumed to occur at an angle φ so as to maximise σ_n. If the micrograins are of the same order of magnitude as the microcracks, the crack orientation would depend on the grain facet distribution.

One of the limitations to this approach is that use is made of the stress field prior to microcracking. It was shown in [33] that the actual process zone is nearly as wide as that estimated by this approach. The estimated zone is 40% longer and variations of the microcrack orientation are also larger. These discrepancies may be used as corrections of the process zone size.

It has been shown in [1,2] that the more distant cracks, with density less than 40% of the saturated condition, contribute less than 3% to the SIF at the macrocrack tip. It is therefore reasonable to reduce the width of the process zone and to neglect those microcracks outside, as shown in Fig. 3.

2.2. Assumptions

The two simplifying assumptions are:

- the fracture toughness K_{IC} is considered a material constant independent of the amount of damage and size of the process zone;
- the saturated density ρ_s is assumed to be independent of the stress level.

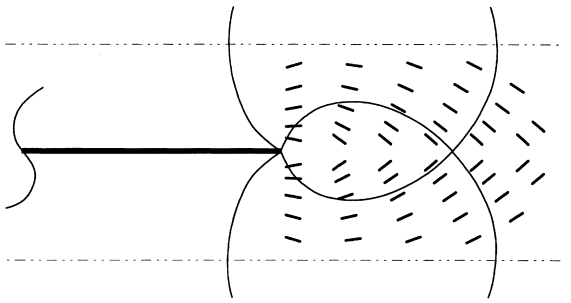

Fig. 3. Partial simulation of the process zone with a distribution of microcracks.

The first assumption implies that K_{IC}, being a macroscopic quantity, stands for the fracture toughness of the homogeneous matrix. Size scale appears to be attributed [6,34] to lower order effects, say at the mesolevel. The second hypothesis seems to be reasonable if the concept of *crack precursor* is accepted [16,33]. Cracks are assumed to nucleate at favorable locations (grain boundaries); they are associated with the material microstructure rather than the macro-stress field. The saturated microcrack density can thus be assumed to coincide with the density of grain facets.

2.3. Microcrack geometry

Fig. 4 displays a system of idealised microcracks where h and S_0 are, respectively, the vertical and horizontal spacing. A mean value d is chosen such that the crack interaction has no effect on the main tip. That is the SIF of the main crack is the same as K_{I0} without the influence of the microcracks. This value is 0.33 times the microcrack half length ℓ.

The microcrack density for the system in Fig. 4 is [2]

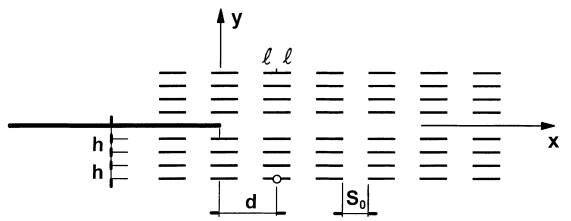

Fig. 4. Geometries with different number of parallel cracks.

Table 1
Microcrack saturated densities for different materials

Material	ρ_s	Reference
Westerly granite	[0.13; 0.16]	[35]
Coconino sandstone	[0.04; 0.06]	[36]
Alumina–zirconia	[0.00; 0.24]	[9]
Silicon-carbide alloy	[0.31; 0.47]	[10]
Concrete	[0.06; 0.20]	[37]

$$\rho = \frac{4\ell^2}{h(S_0 + 2\ell)}, \tag{6}$$

where ℓ is the microcrack half length. Eq. (6) also applies to the case of saturated density, ρ_s. When the geometric parameters are given statistical values, Eq. (6) is no longer applicable for evaluating the local crack density.

Brittle materials are characterised by different microcrack densities according to the material microstructure. Table 1 summarises some experimental data for ceramics, rocks and concrete. The average value for ρ_s is taken equal to 0.25, which is the value used in Eq. (6) subsequently.

2.4. Microcrack distribution

To define a general distribution of microcracks, the orientation $-90° \leqslant \alpha \leqslant 90°$ in Fig. 5 is needed. To simulate random microcracking, the vertical spacing h and the horizontal one S_0 can vary in the ranges $[0.5\ell, 2.0\ell]$ and $[2.5\ell,\ 4.5\ell]$, respectively. This allows local fluctuations of the microcrack density around the mean value of 0.25. The lower bounds of these parameters are used to avoid crack intersection. The microcrack length ranges in the interval $[1/80L,\ 1/20L]$, where L stands for the main crack half length. The upper limit corresponds to cracks in the process zone that origi-

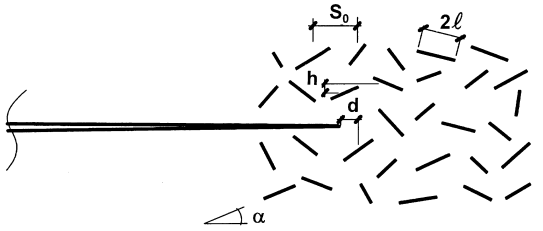

Fig. 5. The five geometric parameters describing the crack distribution inside the process zone.

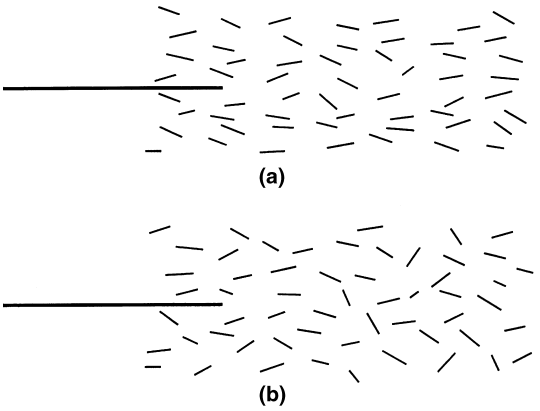

Fig. 6. Disordered distributions of microcracks: (a) Gaussian distribution; (b) uniform statistics.

nate from the coalescence of microcracks. The lower bound corresponds to the limit observed at the mesoscopic scale level. When the microcrack half length is given a statistical distribution, the other parameters have to be referred to the average value of ℓ. Figs. 6(a) and (b) display two disordered Gaussian distributions of microcracks and uniform distribution.

3. Statistical procedure

Under the above-mentioned considerations, different random simulations of microcracks can be set up.

3.1. Gaussian probability

Each geometric parameter can be regarded as a random variable. Complete randomness is obtained by imposing a uniform distribution, while a Gaussian probability density function is suitable for simulating limited fluctuations around a fixed value.

A "*statistical disorder*" can be regarded as "*scattering of data from a mean value*". A uniformly distributed variable is characterised by the maximum scattering; it corresponds to the maximum degree of statistical disorder. A deterministic choice for the variable, which can be thought of as a Dirac-delta distribution, is assumed as an example of minimum disorder. A Gaussian distribution represents a disorder in between the two extremes.

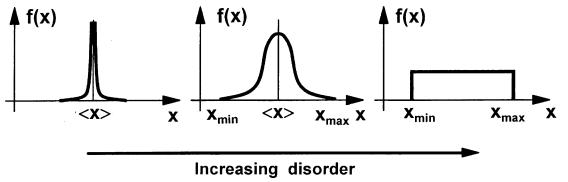

Fig. 7. Statistical distribution and disorder according to various density laws.

The disorder level of the microcrack distribution is illustrated in Fig. 7. Such a statistical approach to a generic distribution of cracks could be applied to describe *statistically disordered* process zones to represent isotropic damage.

For the five independent geometric parameters, a single set of these parameters, representing a distribution of 56 microcracks, involves 56 values of h, S_0, ℓ and α, and a single value of the distance d. They build up a microcrack distribution consisting of 56 microcracks. If these 56 values and the single value for d are defined through a uniform distribution law, then the microcrack distribution corresponds to an isotropic process zone. When the same set of parameters is given a Gaussian probability density function, then the statistical disorder is reduced. The microcracks present only limited fluctuations around their mean values and correspond to anisotropic damage.

The statistical distribution functions have been simulated by means of a Monte Carlo technique. A Gaussian distribution of 80 individuals, for example, is obtained with a skewness coefficient equal to 0.002 and a Kurtosis coefficient equal to 2.77, close to the value of 3 which is typical of an *exact* Gaussian curve (the tails of the curve are terminated in order to keep the random numbers within the range of applicability). A 15% standard deviation of the Gaussian curve is assumed. This represents a distribution law with scattering between the Dirac-delta function and that for uniform distribution.

3.2. Simulation of process zone

A group of 80 simulated process zones is used as a statistical population. Description refers to the average, minimum and maximum K_I at the

main crack tip. Random microcracks are not necessarily symmetric with respect to the macrocrack line. Antisymmetric stress field or K_{II}–SIF could arise.

According to Erdogan and Sih [38], crack growth is assumed to occur in the direction normal to the circumferential stress. In terms of the stress intensity factor quantities, the criterion becomes

$$K_{eq} = \cos\frac{\vartheta}{2}\left(K_I\cos^2\frac{\vartheta}{2} - \frac{3}{2}K_{II}\sin\vartheta\right) = K_{IC}. \qquad (7)$$

Consider a group of microcracks of constant length ℓ and regard the parameters d, h and α as random variables. The horizontal spacing S_0 is determined via Eq. (6) once h and ℓ are known. This means that, if ℓ is given a fixed value, S_0 is a random variable with the same statistics as h. Three different statistics are considered:

Case A. All parameters are given a Dirac-delta distribution (a deterministic choice inducing highly anisotropic damage).

Case B. All parameters are defined by a Gaussian curve.

Case C. A uniform distribution function is coupled with all the parameters (isotropic damage).

For each of the second and third choice, a series of 80 simulations has been made. The results are plotted in Fig. 8. Fig. 8(a) shows that the average SIFs, both K_I and K_{eq}, decrease as the statistical disorder of the microcracks is increased. A Gaussian distribution around the mean value (group G) produces a shielding effect which is 10% of the reference value on the average. A further increase of disorder obtained through the uniform distribution law for every parameter (Case C) leads to more pronounced shielding effect up to 20% of the remotely applied SIF K_{I0} that can be calcualted for the macrocrack in absence of microcracks. Broken lines correspond to the maximum and minimum SIFs found at the main crack tip among the 80 samples. It can be seen that some microcrack arrangement produces a strong amplification (40% of K_{I0}), while others may yield a strong shielding (70% of K_{I0}).

Fig. 8(b) shows that the global average of shielding on the main crack is not due to the influence of few samples, but it is a general trend of the entire population.

An analogous trend is shown in Fig. 9 for the situation when the microcracks are parallel to the main crack and the assumption of constant crack density is removed. The rest of the parameters are given according to a Dirac-delta distribution, a Gaussian probability density function, and a uniform distribution.

Consider a partially disordered crack distribution where the parameters d, α and S_0 are given a

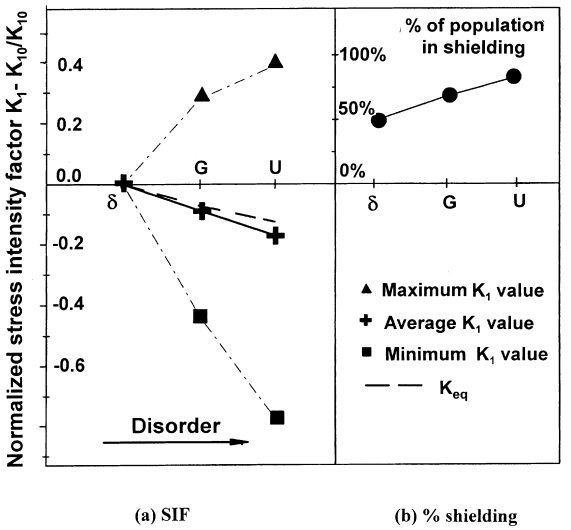

Fig. 8. Statistically disordered populations on d, α and h.

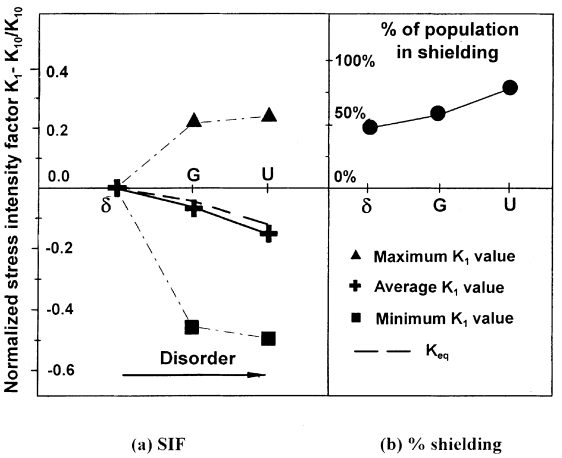

Fig. 9. Statistically disordered populations on S_0, h and d.

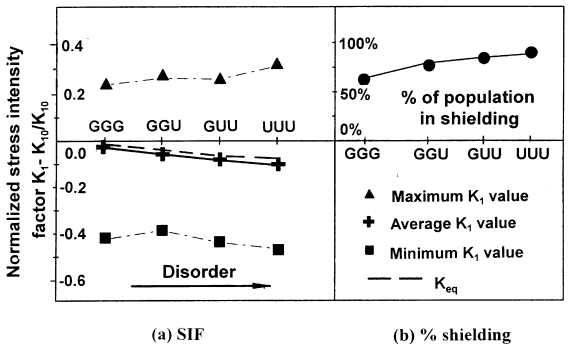

Fig. 10. Statistically disordered populations on d, α and S_0.

Gaussian distribution, while ℓ is kept constant. A population of 80 specimens indicated as group GGG is shown in Fig. 10. The disorder is reflected via a uniform statistical distribution of the spacings S_0 and h via Eq. (6). The remaining parameters maintain the Gaussian probability function (group GGU). More disorder would result if the other Gaussian distributions are changed to uniform distributions. The group GUU in Fig. 10 reflects change of α. When all the three parameters are changed, the results correspond to UUU.

Again, shielding is increased as disorder is introduced. The average SIF is 12–13% lower than K_{I0}. Again, this effect is a trend of the entire population, Fig. 10(b).

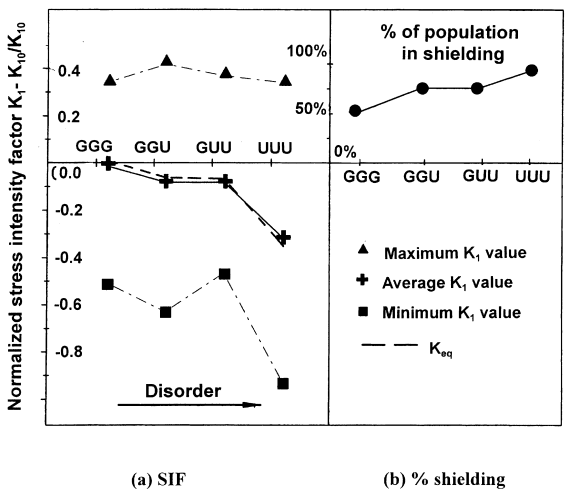

Fig. 11. Statistically disordered populations on h, S_0 and d.

Analogous trends are summarised in Fig. 11. They differ from those discussed earlier, since the microcracks are kept parallel to the main crack and their length takes different values.

4. Discussion and conclusion

The results presented account for 960 numerical simulations and the test of more than 4000 specimens [39]. Assuming that K_{IC} is a material parameter of constant value, the average shielding effect on the main crack turns out to be approximately 20% of K_{I0}.

In [16] the shielding of the main crack by the microcrack process zone has been estimated to be $0.92\rho_s$ to $1.15\rho_s$ according to different crack nucleation criteria. The present study estimates ρ_s to be 0.25 on the average. This corresponds to a mean shielding of the main crack of 23–28% of K_{I0}. Taking into account a group of non-interacting microcracks, a global shielding effect of about 1.61 times the saturated density is found [16]. For the microcrack density considered, this yields 40% of K_{I0} which is twice the present result. The difference can be explained as follows:

- In [16], the author considers the microcracks to be oriented in the principal tensile stress direction. The present study considers the microcracks to be oriented randomly or parallel to the main crack.
- Mutual interactions between the microcracks are neglected in [16]. This could lead to an underestimate of the result.

Good agreement is found for the theoretical and experimental data in [10]. For a stationary crack under static loading, the shielding effect is estimated to be 25% of K_{I0}.

This work is similar to the approach in [40–43], but the results are different. The numerical simulations in [40–43] are limited to six specimens related to random distributions of microcracks with constant length. Microcracks had no statistically stable effect on the main crack. The same conclusion is obtained for microcracks oriented in the principal stress directions. Six specimens are not sufficient to estabilish a statistical base.

In all the simulations of this work, the microcracks seldom experience an equivalent SIF that is higher than K_{eq} at the main crack tip. Even though microcrack propagation and coalescence could take place, nevertheless it is the macroscopic crack that is responsible for the global cracking phenomenon. This view differs from that in [23].

Acknowledgements

The authors gratefully acknowledge the financial support of the National Research Council (CNR) and the Department for University and Scientific and Technological Research (MURST). Thanks are also due to the European Community for the TMR Contract ERBFMRXCT 960062.

References

[1] A. Brencich, A. Carpinteri, Interaction of a main crack with ordered distributions of microcracks: a numerical technique by displacement discontinuity boundary elements, Int. J. Fracture 76 (1996) 373–389.
[2] A. Brencich, A. Carpinteri, Stress field interaction and strain energy distribution between a stationary main crack and its process zone, Eng. Fracture Mech. 59 (1998) 797–814.
[3] R.G. Hoagland, G.T. Hahn, A.R. Rosenfield, Influence of microstructure on fracture propagation in rock, Rock Mech. 5 (1973) 77–106.
[4] N. Claussen, Fracture toughness of Al_2O_3 with an unstabilized ZrO_2 dispersed phase, J. Am. Ceram. Soc. 59 (1976) 49–51.
[5] K.T. Faber, A.G. Evans, Crack deflection processes – II. Experiment, Acta Metallurgica 4 (1983) 577–584.
[6] X.Z. Hu, F.H. Wittmann, Fracture energy and fracture process zone, Mater. Struct. 25 (1992) 319–326.
[7] F.H. Wittmann, V. Slowik, A.M. Alvaredo, Probabilistic aspects of fracture energy of concrete, Mater. Struct. 27 (1994) 499–504.
[8] M. Rühle, N. Claussen, A.H. Heuer, Transformation and microcrack toughening as complementary processes in ZrO_2-toughened Al_2O_3, J. Am. Ceram. Soc. 69 (1986) 605–697.
[9] M. Rühle, A.G. Evans, R.M. McMeeking, P.G. Charalambides, J.W. Hutchinson, Microcrack toughening in alumina/zirconia, Acta Metallurgica 35 (1987) 2701–2710.
[10] L.X. Han, S. Suresh, High-temperature failure of an alumina-silicon carbide composite under cyclic loads: mechanisms of fatigue crack tip damage, J. Am. Ceram. Soc. 72 (1989) 1233–1238.
[11] W. Kreher, W. Pompe, Increased fracture toughness of ceramics by energy-dissipative mechanisms, J. Mat. Sci. 16 (1986) 694–706.
[12] A.G. Evans, Y. Fu, Some effects of microcracking on the mechanical properties of brittle solids – II. Microcrack toughening, Acta Metallurgica 8 (1985) 1525–1531.
[13] D.R. Clarke, A simple calculation of process zone toughening by microcracks, Comm. Am. Ceram. Soc. (1984) C15–C16.
[14] J.W. Hutchinson, Crack tip shielding by micro-cracking in brittle solids, Acta Metallurgica 35 (1987) 1609–1619.
[15] S.X. Gong, S.A. Meguid, On the effect of the release of residual stresses due to near-tip microcracking, Int. J. Fracture 52 (1991) 257–274.
[16] S.X. Gong, On the formation of near-tip microcracking and associated toughening effects, Eng. Fracture Mech. 50 (1995) 29–39.
[17] K.T. Faber, A.G. Evans, Crack deflection processes – I. Theory, Acta Metallurgica 4 (1983) 565–576.
[18] M. Ortiz, Microcrack coalescence and macroscopic crack growth initiation in brittle solids, Int. J. Sol. Struct. 24 (1988) 231–250.
[19] A. Dolgopolsky, V. Karbhari, S.S. Kwak, Microcrack induced toughening – an interaction model, Acta Metallurgica 37 (1987) 1349–1354.
[20] A. Carpinteri, C. Scavia, Order and disorder in microcrack distribution: effects on macrocrack behaviour and maximum load, in: J.G.M. Van Mier, J.G. Rots, A. Bakker (Eds.), Proceedings of the International RILEM/ESIS Conference on Fracture Processes in Brittle Disordered Materials: Concrete, Rock, Ceramics, Dordrecht, vol. 1, E&FN Spon, Noordwijk, 1991, pp. 1173–1182.
[21] M. Ortiz, A continuum theory of crack shielding in ceramics, J. Appl. Mech. 54 (1987) 54–58.
[22] B. Budiansky, J.W. Hutchinson, J.C. Lambropoulos, Continuum theory of dilatant transformation in ceramics, Int. J. Sol. Struct. 19 (1983) 337–355.
[23] K.M. Shum, J.W. Hutchinson, On toughening by microcracks, Mech. Mater. 9 (1990) 83–91.
[24] A. Misra, A.A. Sukere, Micro-crack toughening in particulate composites, Int. J. Fracture 52 (1991) R37–R44.
[25] M. Kachanov, E.L. Montagut, J.P. Laures, Mechanics of crack–microcrack interactions, Mech. Mater. (1990) 59–71.
[26] A.A. Rubinstein, Macrocrack interaction with semi-infinite microcrack array, Int. J. Fracture 27 (1985) 113–119.
[27] A.A. Rubinstein, H.C. Choi, Macrocrack interaction with transverse array of microcracks, Int. J. Fracture 36 (1988) 15–26.
[28] M. Kachanov, E.L. Montagut, Interaction of a crack with certain microcrack arrays, Eng. Fracture Mech. 25 (1986) 625–636.
[29] M. Kachanov, Elastic solids with many cracks: a simple method of analysis, Int. J. Sol. Struct. 23 (1987) 23–43.
[30] J.R. Bristow, Microcracks and the static and dynamic elastic constants of annealed and heavily cold-worked metals, Brit. J. Appl. Phys. 11 (1960) 81–95.
[31] J.B. Walsh, The effect of cracks on the compressibility of rocks, J. Geophys. Res. 70 (1965) 381–389.

[32] M. Kachanov, Elastic solids with many cracks and related problems, Adv. Appl. Mech. 30 (1993) 259–445.
[33] R.G. Hoagland, J.D. Embury, D.J. Green, On the density of microcracks formed during the fracture of ceramics, Scripta Metallurgica 9 (1973) 907–909.
[34] A. Carpinteri, B. Chiaia, Size effects on concrete fracture energy: dimensional transition from order to disorder, Mater. Struct. 29 (1996) 259–266.
[35] K. Hadley, Comparison of calculated and observed crack densities and seismic velocities in Westerly granite, J. Geophys. Res. 81 (1976) 3484–3494.
[36] M.A. Gawad, J. Bulan, B. Tittmann, Quantitative characterisation of microcracks at elevated pressures, J. Geophys. Res. 92 (1987) 12,911–12,916.
[37] K.M. Nemati, P.J.M. Monteiro, Effect of confinement on the fracture behaviour of concrete under compression, in: F.H. Wittmann (Ed.), Proceedings of FRAMCOS-2, Second International Conference on Fracture Mechanics of Concrete and Concrete Structures, Zürich, 1995, vol. III, Aedificatio, Freiburg, 1996, pp. 1843–1852.
[38] F. Erdogan, G.C. Sih, On the crack extension in plates under plane loading and transverse shear, J. Basic Eng. 85 (1963) 519–527.
[39] A. Brencich, Interaction of a main crack with a disordered distribution of microcracks, Ph.D. Thesis, Department of Structural Engineering, Politecnico di Torino, 1996 (in Italian).
[40] E. Montagut, M. Kachanov, On modelling a microcracked zone by ''weakened'' elastic material and on statistical aspects of crack–microcrack interactions, Int. J. Fracture 37 (1988) R55–R62.
[41] M. Kachanov, J.P. Laures, Strong three-dimensional interactions of several arbitrary located penny-shaped cracks, Int. J. Fracture 37 (1988) R63–R68.
[42] M. Kachanov, J.P. Laures, Three dimensional problems of strongly interacting arbitrary located penny-shaped cracks, Int. J. Fracture 41 (1989) 289–313.
[43] J.P. Laures, M. Kachanov, Three dimensional interactions of a crack front with arrays of penny-shaped microcracks, Int. J. Fracture 48 (1991) 255–279.